ICSV30 AMSTERDAM 8-11 JULY 2024

VIRTUAL SENSING FOR ACTIVE NOISE CONTROL IN AIRCRAFT

Ioanna Vasilakopoulou-Trapali
German Aerospace Center, Institute of Composite Structures and Adaptive Systems, Braunschweig, Germany.
E-mail: Ioanna.vasilakopoulou-trapali@dlr.de
Malte Misol
German Aerospace Center, Institute of Composite Structures and Adaptive Systems, Braunschweig, Germany.
E-mail: Malte.Misol@dlr.de
Hans Peter Monner
German Aerospace Center, Institute of Composite Structures and Adaptive Systems, Braunschweig, Germany..
E-mail: Hans.Monner@dlr.de
Manfred Nader
Linz Center of Mechatronics GmbH, Linz, Austria
E-mail:manfred.nader@lcm.at

This paper focuses on the initial phase of designing a robust active noise control (ANC) system customized for aircraft cabin environments, using virtual sensors. This involves incorporating monitoring sensors and additional filters into the controller. Previous research has shown that ANC systems with remote sensors are highly sensitive to changes in the physical plants. The primary variations within an aircraft cabin originate from passenger presence, cargo, and cabin crew equipment, which can significantly impact system performance and stability. This study emphasizes the importance of evaluating the effects of such perturbations on the ANC system and applying predictive techniques to anticipate their influence without exhaustive measurement. The superposition method is explored to address different perturbation combinations, utilizing a simplified laboratory setup in a fully anechoic environment. The objective is to assess various perturbation combinations within the anechoic chamber, using different objects with reflective and absorptive surfaces, aiming to understand predictability across various scenarios using the superposition approach.

Keywords: active noise control, virtual sensors, uncertainties, superposition

1. Introduction

Local active noise control systems aim to create a localised zone of quiet at the physical error sensor by minimising the acoustic pressure at the physical error sensor location with secondary sound sources. Although substantial noise reduction can be accomplished at the physical sensor location, the resulting quiet zone typically remains limited in size [1]. Due to the confined nature of the quiet zone formed around the physical error sensor, especially within a sphere with a diameter equivalent to one-tenth of the excitation wavelength, virtual error sensors have been introduced. In the case of virtual sensing the number of error sensors can be easily increased as the number of physical sensors and the numbers of additional filters are not influenced. These virtual error sensors serve to relocate the quiet zone to a specified location that is situated away from the physical sensors [2]. The virtual algorithms estimate the noise signal at the passenger's ear or virtual microphone location using the noise signal at the physical microphones placed away from the ears [3].

The robustness of the performance of these systems is dependent on the type of uncertainties in the plant responses [4], [5]. In previous publications, the smart lining concept, as proposed by Misol et al. [6], [7] investigates the integration of structural sensors in the virtual sensing algorithms. As it was demonstrated the choice of virtual sensors introduce a feedback path into the control plant which is very sensitive to changes in the acoustic enclosure. This previous work investigates the effect of environmental changes in the acoustic domain, highlighting the degradation in control performance when there is a temperature disparity between the structural secondary path and the real-time control temperature. It has been demonstrated that temperature compensation for the secondary path model in the *Remote Microphone technique* is essential, as the performance and stability are strongly affected [6].

The subsequent publication aims to establish the impact of uncertainties like seat occupancy's and the presence of different reflective surfaces, which is considered dominant during flight operations. With this type of interference, scenarios can occur simultaneous in which it would be impossible to measure all possible different combinations. As demonstrated by Elliot et al. [8], the uncertainty linked to these perturbations can be estimated using the superposition method, which accounts for the uncertainties associated with each perturbation occurring independently. This is closely tied to the inherent reflective characteristic of these perturbations, which has been demonstrated to be cumulative. The idea can be effectively used in the acoustic domain of a commercial aircraft cabin, as different uncertainty scenarios are occurring constantly and simultaneously.

Under the assumption that the dominant characteristic of these perturbations is their reflective nature, this paper aims to design a simplified experimental setup to quantify the maximum deviations in plant responses from nominal conditions to various perturbations within a zero anechoic boundary condition. By measuring the individual plant responses of different objects in the anechoic chamber and then assessing their possible combinations, the actual measured responses are compared with the expected values based on the superposition method of the uncertainties. In this paper, the validity of the method is demonstrated in accurately predicting the behavior of various combinations of objects within the acoustic environment in the majority of cases tested. However, weaknesses in the method are also identified due to the interactions of the acoustic waves between the objects.

2. Additive Uncertainty

Assuming $G_0(j\omega)$ describes the unperturbed nominal condition in the frequency domain, every frequency response function (FRF) can be structured as a combination of the nominal part and the part of the additive uncertainty $\Delta G(j\omega)$ [4]. In case of two different individual perturbations the FRF can be described as:

$$G_1(j\omega) = G_0(j\omega) + \Delta G_1(j\omega) \tag{1}$$

$$G_2(j\omega) = G_0(j\omega) + \Delta G_2(j\omega) \tag{2}$$

With the combination of these two individual perturbations, another frequency response will occur:

$$G_{12}(j\omega) = G_0(j\omega) + \Delta G_{12}(j\omega) \tag{3}$$

In Equation (3), $\Delta G_{12}(j\omega)$ is the additive uncertainty when the two individual perturbations are occurring simultaneously. As the number of individual perturbations increases, the variety of combinations also grows, resulting in a potentially large number of required measurements. To avoid that expense, a possible method for predicting the additive uncertainty of the different combinations is the method of superposition. The estimated additive uncertainty in Equation (3) can be expressed as:

$$\Delta\widetilde{G}_{12}(j\omega) = \Delta G_1(j\omega) + \Delta G_2(j\omega) \tag{4}$$

Based on the superposition method, the estimated frequency response function of the combined uncertainty can be written as:

$$\widetilde{G}_{12}(j\omega) = G_0(j\omega) + \Delta\widetilde{G}_{12}(j\omega) \tag{5}$$

3. Methods

3.1 Experimental setup

In Figure 1, a scheme of the laboratory setup in the anechoic room of the Otto-von-Guericke-Universität Magdeburg is shown with the respective dimensions. The four loudspeakers are arranged in the corners of the anechoic room and nine microphones are hanging from the ceiling. This first configuration in Figure 1 can be assessed as the nominal condition and the unperturbed plant responses from the four loudspeakers to the nine microphones are being measured every day prior to the perturbed measurements. The time data which needed for the calculation of the frequency response functions (FRF) from the loudspeakers to the microphones are obtained from a multi-reference test. The acoustic load case is realized by driving the four loudspeakers with uncorrelated band-limited white noise signals up to 1 kHz.

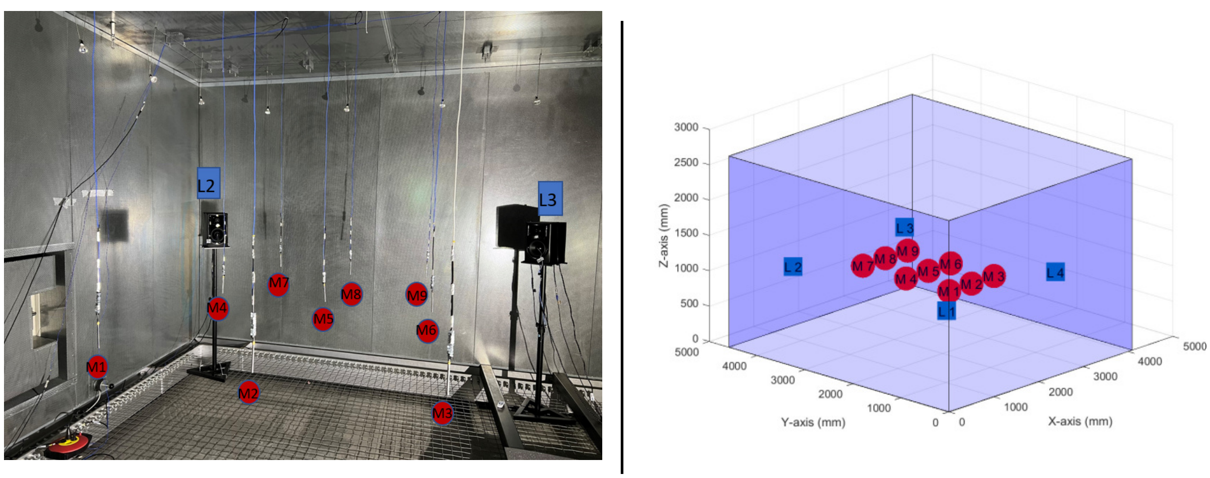

Figure 1: The experimental setup in the anechoic room equipped with the loudspeakers *L1, L2, L3, L4* and the microphones *M1, M2, M3, M4, M5, M6, M7, M8, M9*. The loudspeakers membranes point into the direction of the center of the microphone *M5*.

For experimentally determining the additive uncertainty $\Delta G(j\omega)$, repeated measurements of perturbed systems are necessary [9]. To simulate perturbations with a reflective nature, different objects are positioned inside the anechoic chamber. Table 1 provides a detailed overview of the 10 perturbations employed during the experimental phase. Measurements of the responses between the loudspeakers and the microphones were conducted with the 10 uncertainties individually, and then 4 possible combinations of them were selected. In the next section the effects of the combined perturbations in these 4 different scenarios will be presented and compared with the predicted results from the superposition method.

Cases	Perturbations	Combinations
1.	Box 1 in the center	Combination 1
2.	Box 2 in the center	
3.	Move Box 1 forwards	Combination 2
4.	Move Box 2 backwards	
5.	Box 3 in the center	
6.	Aircraft seat row with Person 1 in the left seat	Combination 3
7.	Aircraft seat row with Person 2 in the right seat	
8.	Aircraft seat row with Box 1 in the left seat	Combination 4
9.	Aircraft seat row with Box 2 in the right seat	
10.	Aircraft seat row with Person 1 in the middle seat	

Table 1: List of the 10 individual perturbations used for the measurement of the additive uncertainty in the plant responses from the loudspeakers to the microphones and their combinations.

3.2 Analysis

For each case, the phase and the magnitude of the frequency responses are measured individually for each perturbation, as well as for their combined effects. In the low-frequency range (up to 500 Hz) that's crucial for the active noise control systems, it is important to assess the changes that different objects cause. Even if these changes are subtle, because the acoustic wavelength of the source is large in comparison with the object dimensions, they should be quantified and their influence on the robustness of the ANC system should be assessed.

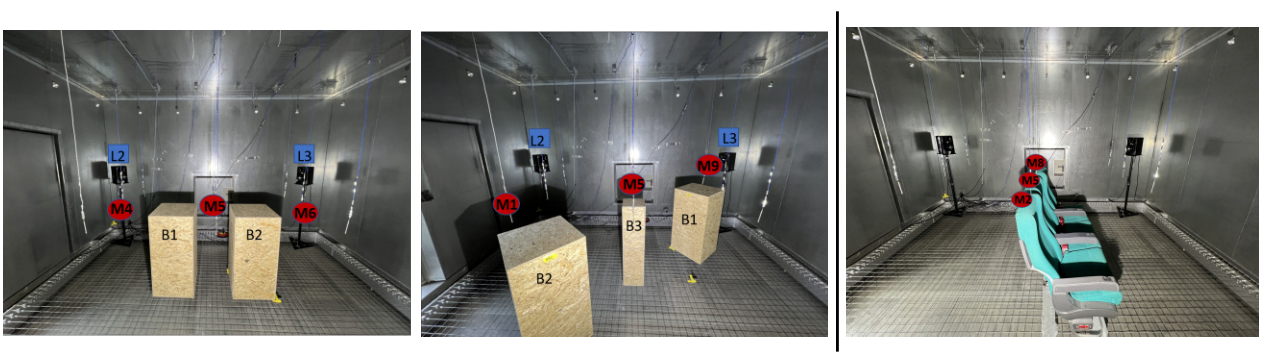

a. b.

Figure 2: a) The experimental setup with Combination 1 and Combination 2, from Table 1. Combination 1 includes Box 1 positioned between microphones M4 and M5 and Box 2 between M5 and M6, aligned with the center of the anechoic chamber. Combination 2 includes Box 1 positioned below microphone M9, Box 2 below M1, and Box 3 below M5. b) The aircraft seat row, with left seat below microphone M8, middle seat below M5, and right seat below M2 for cases 6-10, from Table 1.

Figure 3 shows the magnitude and the phase of the frequency response measured from loudspeaker *L3* to microphone *M1* under four different conditions, including the nominal condition, case 1, case 2 and *Combination 1*, as presented in Table 1. Figure 2a shows the combined scenario of this case in the anechoic chamber before the measurement of the perturbed frequency response. At 622 Hz a maximum deviation of 11.6 dB is observed between case 1 and the combined perturbation. In Figure 4 the magnitude and the phase of the combined perturbation from Figure 3 are compared, with the predicted values calculated from Equation (3),(5). It can be seen that there is good alignment, in both magnitude and phase, between the uncertainties due to the two perturbations. The maximum change in magnitude is up to 4 dB, in Figure 4a and up to 10 degrees in phase, in Figure 4b.

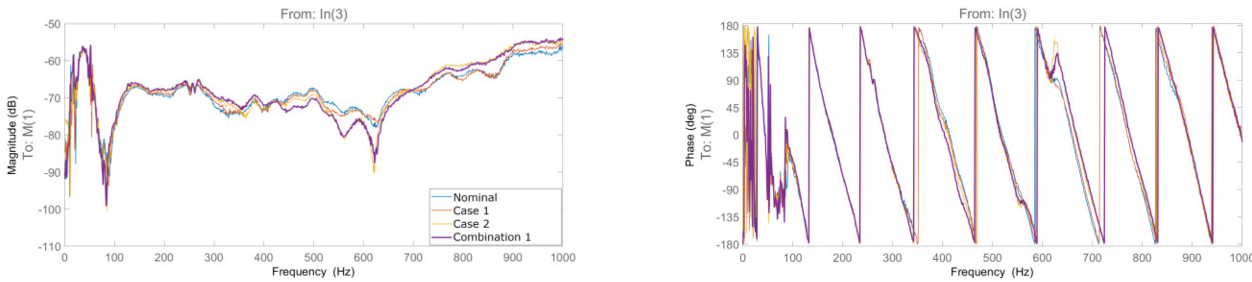

a. b.

Figure 3: *The frequency response from loudspeaker L3 to microphone M1, for case 1 and case 2, from Table 1, compared with the nominal condition and the combined perturbations.*

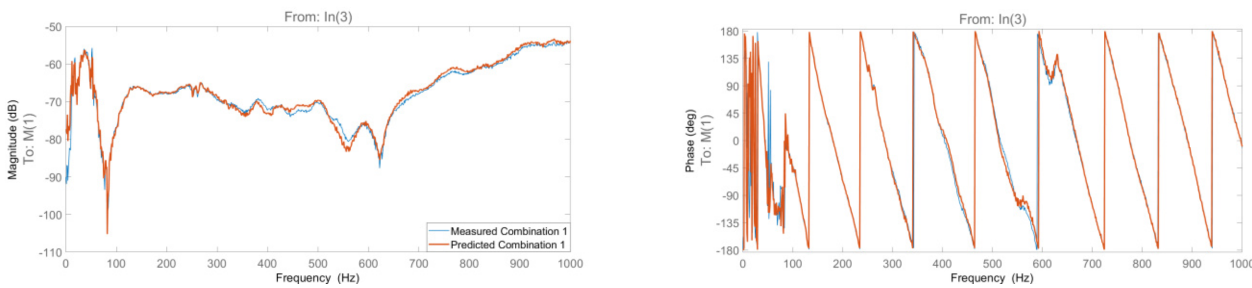

a. b.

Figure 4: *The measured frequency response for Combination 1, as shown in Table 1, compared with the predicted case, as computed from the sum of the two individual perturbation, from cases 1 and 2.*

The next analysis case, involves five different conditions. In Figure 5 the cases 3,4 and 5, the nominal condition and *Combination 2* are presented, as noted in Table 1. The detailed locations of the boxes for this experimental setup are presented in Figure 2a. In Figure 5a, a resonance is observed in the frequency response of the combined perturbation at 250 Hz with a maximum difference of 17dB from the individual perturbations. This abrupt change could be attributed to the formation of standing waves between the three objects. For the prediction method three different additive uncertainties $\Delta G_1(j\omega)$, $\Delta G_2(j\omega)$, $\Delta G_3(j\omega)$ are computed for cases 3, 4, and 5. In this case the results reveal a weakness for the prediction method. The predicted curve in Figure 6, shows a difference of 17dB at the same frequency. This consistency suggests that the observed peak is solely due to the interaction of waves within the combined perturbation scenario and does not originate from the individual responses of the objects. There is also observed a phase difference of 80 degrees at 250 Hz, that can cause instabilities in the ANC system. It seems that in *Combination 2*, the superposition method is not as applicable.

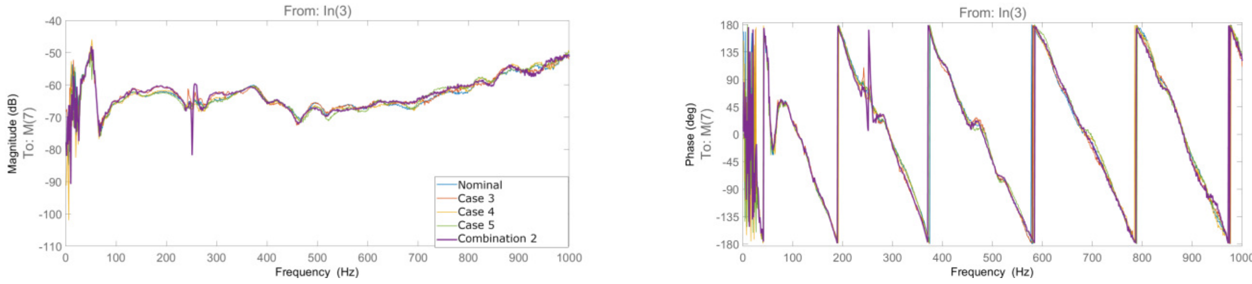

a. b.

Figure 5: *The frequency response from loudspeaker L3 to microphone M7, for three individual perturbations, case 3,4,5 from Table 1, compared with the nominal condition and the combined perturbation.*

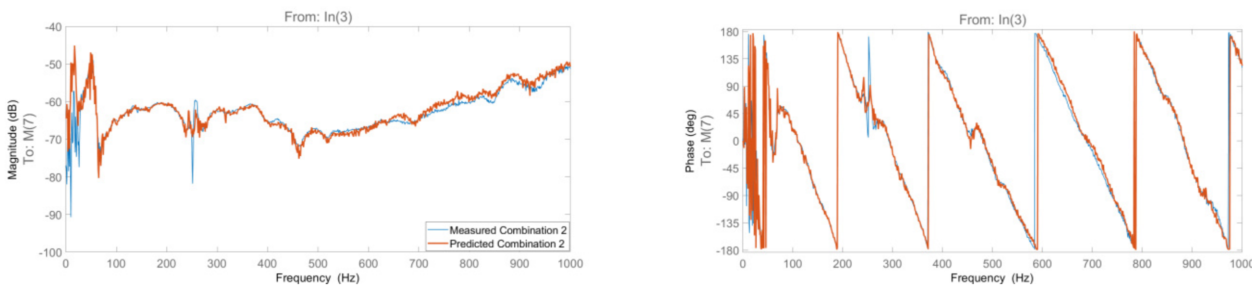

a. b.

Figure 6: *The measured frequency response for Combination 2, as shown in Table 1, compared with the predicted case, as computed from the sum of the three individual perturbations, from cases 3, 4 and 5.*

For the next set of measurements, the perturbations within the aircraft seat row are presented. The unperturbed measurements are repeated in this case, with the anechoic chamber containing the aircraft seat row placed below the central row of microphones, as presented in Figure 2b. This condition is assessed as the nominal one. The perturbed cases in this measurement involve introducing objects on the aircraft seats. Figure 7 shows the acoustic responses of the individual cases 6, and 7 from Table 1, and *Combination 3*. This case simulates an aircraft cabin environment with two people seated in the aircraft seat row, and the microphone configuration positioned at the ear height. The maximum magnitude difference observed in Figure 8a is 7 dB at 366 Hz for the lower frequency range, while a deviation of 13.6 dB is observed at 836 Hz.

The measured and predicted acoustic responses for *Combination 4* are presented in Figure 9. There is a maximum difference of 4 dB at 445 Hz in magnitude and 28 degree in phase at 248 Hz. The close agreement here, can be viewed as a promising outcome for the superposition method, particularly for its applicability to surfaces that are not so reflective, such as the human body and the absorbent surface of the aircraft seat row.

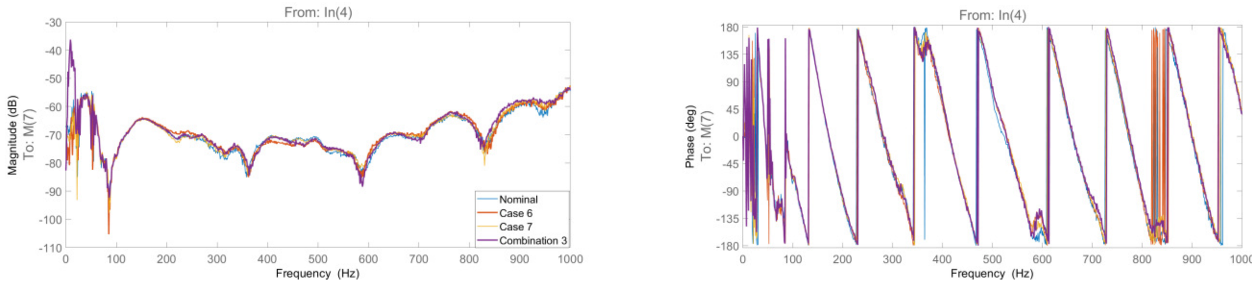

a. b.

Figure 7: *The frequency response from loudspeaker L4 to microphone M7 for the nominal condition, cases 6,7, and Combination 3 from Table 1.*

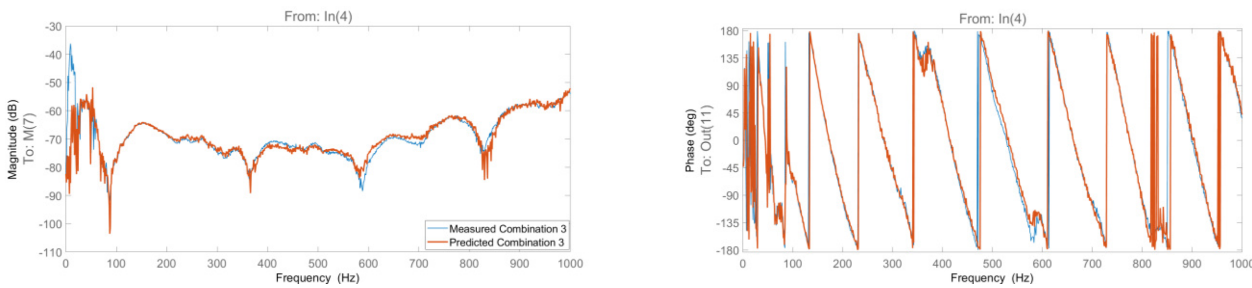

a. b.

Figure 8: *The measured frequency response for Combination 3, as shown in Table 1, compared with the predicted case, as computed from the sum of the two individual perturbation, from cases 6 and 7.*

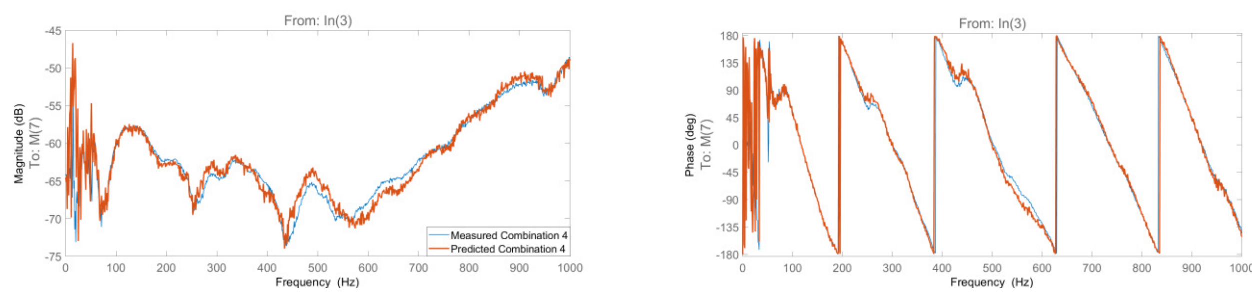

a. b.

Figure 9: *The measured frequency response for Combination 4, as shown in Table 1, compared with the predicted case, as computed from the sum of the three individual perturbation, from cases 8,9 and 10.*

4. Conclusions

This study investigates the impact of uncertainties on the plant responses of four distinct systems under combined perturbations. Employing the superposition of additive uncertainties, the frequency responses of these systems based on individual uncertainties are predicted. While this method has demonstrated reasonable accuracy for simpler systems, primarily influenced by diffraction and reflection of acoustic waves, significant deviations of more than 10 dB in magnitude and 80 degree in phase exist in a scenario that is dealing with more than two objects. This suggests limitations in its applicability to more complex scenarios where acoustic wave interactions with multiple objects complicate the system. To validate the efficacy of the method, further research is essential. This demands developing parametric acoustic simulations capable of extending beyond this experimental setups, to study more complicate systems with diverse perturbations within a cavity. Apart from that, the measured plant responses for the 10 perturbations should be also tested in ANC algorithms, to assess their stability and robustness under different operating conditions of the acoustic environment.

5. Acknowledgments

The project was carried out in the framework of the European Union's Horizon Europe programme IN-NOVA MSCA Doctoral Network under the Marie Sklodowska-Curie grant agreement number 10107303 and has been supported by the LCM – K2 Center within the framework of the Austrian COMET-K2 programme.

REFERENCES

1. Dunant Halim, Li Cheng, and Zhongqing Su. Virtual sensors for active noise control in acoustic–structural coupled enclosures using structural sensing: robust virtual sensor design. *The Journal of the Acoustical Society of America*, 129(3):1390–1399, 2011.

2. Danielle J. Moreau, Benjamin S. Cazzolato, Anthony C. Zander, and Cornelis Petersen. A review of virtual sensing algorithms for active noise control. *Algorithms*, 1:69–99, 2008.

3. Stephen Elliott, Chung Kwan Lai, Thibault Vergez, and Jordan Cheer, editors. *Robust stability and performance of local active control systems using virtual sensing*, Berlin, 2019. Deutsche Gesellschaft für Akustik.

4. K.H. BAEK and S.J. ELLIOTT. The effects of plant and disturbance uncertainties in active control systems on the placement of transducers. *Journal of Sound and Vibration*, 230(2):261–289, 2000.

5. Jin Zhang, Stephen Elliott, and Jordan Cheer. Robust performance of virtual sensing methods for active noise control. *Mechanical Systems and Signal Processing*, 152, May 2021.

6. Malte Misol, Stephan Algermissen, Michael Rose, and Hans Peter Monner. Aircraft lining panels with low-cost hardware for active noise reduction. In *Proceedings of Joint Conference ACOUSTICS 2018*, 2018.

7. Malte Misol and Stephan Algermissen. Remote sensing for a lining integrated active structural acoustic control system. In *9th EASN International Conference*, September 2019.

8. Stephen J. Elliott, Jin Zhang, Chung Kwan Lai, and Jordan Cheer. Superposition of the uncertainties in acoustic responses and the robust design of active control systems. *The Journal of the Acoustical Society of America*, 148 3:1415, 2020.

9. Kay Kochan, Eugen Weizel, and Delf Sachau, editors. *Evaluation of the Stability and Performance of an uncertain Active Noise Control System*. Institute of Noise Control Engineering - USA (INCE-USA), 2009.